AD/A-002 374

THE FAR INFRARED AND SUBMILLIMETER BACKGROUND

James R. Houck, et al

Cornell University

Prepared for:

Air Force Cambridge Research Laboratories
Defense Advanced Research Projects Agency

15 March 1974

UNCLASSIFIED

Security Classification

AD/A-002 374

DOCUMENT CONTROL DATA - R & D

(Security classification of title, body of abstract and indexing annotation must be entered when the overall report is classified)

1. ORIGINATING ACTIVITY (Corporate author)
Cornell University
Center for Radiophysics and Space Research
Ithaca, New York 14850

2a. REPORT SECURITY CLASSIFICATION
Unclassified

2b. GROUP

3. REPORT TITLE

THE FAR INFRARED AND SUBMILLIMETER BACKGROUND

4. DESCRIPTIVE NOTES (Type of report and inclusive dates)

Scientific. Final, 15 Novemver 1969 - December 31 1973 Approved 6 May 1974

5. AUTHOR(S) (First name, middle initial, last name)
James R. Houck
Baruch T. Soifer
Martin O. Harwit
Judith L. Pipher

6. REPORT DATE
15 March 1974

7a. TOTAL NO. OF PAGES
62

7b. NO. OF REFS
55

8a. CONTRACT OR GRANT NO. DARPA
F19628-70-C-0128

b. PROJECT NO., Task, Work Unit Nos.
1366 n/a n/a

c. DoD Element 62301D

d. DoD Subelement n/a

9a. ORIGINATOR'S REPORT NUMBER(S)

9b. OTHER REPORT NO(S) (Any other numbers that may be assigned this report)
AFCRL TR-74-0202

10. DISTRIBUTION STATEMENT

A- Approved for public release; distribution unlimited.

11. SUPPLEMENTARY NOTES
This research was supported by the Advanced Research Projects Agency.

12. SPONSORING MILITARY ACTIVITY
Air Force Cambridge Research Laboratories (OP)
Hanscom AFB, Massachusetts 01731
Contract Monitor: Stephan D. Price/OPI

13. ABSTRACT

During the period of the contract Cornell has prepared and successfully flown three liquid Helium cooled infrared telescopes. The major accomplishments of this program are described in the first four sections of this report. The fifth section reports a ground based photometer designed and built under this program.

I. The first measurement of thermal radiation from zodiacal particles at wavelengths longer than 5μ.

II. The first measurements of diffuse thermal emission from the plane of our galaxy.

III. The mapping of many sources in the plane of the galaxy including the galactic center at 5, 10, 20 and 100μ.

IV. Measurement of the diffuse sky background radiation in the submillimeter region of the spectrum.

V. Groundbased infrared astronomy program.

DD FORM 1 NOV 65 1473

Unclassified

Security Classification

14. KEY WORDS	LINK A		LINK B		LINK C	
	ROLE	WT	ROLE	WT	ROLE	WT
INFRARED						
SUBMILLIMETER						
BACKGROUND						

1a

TABLE OF CONTENTS

Section I. ROCKET INFRARED OBSERVATIONS OF THE INTERPLANETARY MEDIUM

Baruch T. Soifer++, J. R. Houck*, and Martin Harwit

ABSTRACT

Upper limits on the diffuse background radiation in the intermediate infrared ($5\mu \leq \lambda \leq 23\mu$), as measured from a sounding rocket, are presented. Evidence is given for the detection of thermal emission from the interplanetary medium.

++ Now at University of California, San Diego

* Alfred P. Sloan Research Fellow

Preceding page blank

Introduction

On 2 December 1970 a liquid helium cooled telescope was carried to a peak altitude of 190 km by an Aerobee 170 rocket from White Sands, New Mexico. This paper reports the observed background for the three short wavelength detectors ($5\mu \leq \lambda \leq 23\mu$). A comparison of the observations and models of the interplanetary medium is presented. Pipher et al. (1971) have discussed the observed backgrounds for $60\mu < \lambda < 1500\mu$.

The optical system consists of a prime focus telescope D = 6.75", f = 0.9, and is described in detail elsewhere (Pipher et al., 1971; Harwit, Houck, Fuhrmann, 1969). The three short wavelength detectors flown were copper-doped germanium photoconductors fabricated in the manner described by Quist (1968). The spectral bandpasses were defined by the characteristic Ge:Cu response and interference and blocking filters. The spectral response of each detector-filter system was measured using a Perkin Elmer 301 Far Infrared Spectrophotometer. The sensitivity of the systems in the flight telescope was determined by the calibration procedure described by Harwit, Houck, and Fuhrmann (1969). Absolute calibration errors are difficult to determine. We believe, however, that our undertainties are less than a factor of 2. The first three columns of Table I give the wavelength ranges and sensitivities of these detectors. Also included is the same data for one of the submillimeter detectors, a Ge:Ga photoconductor.

The Flight

The rocket was launched at 01:32 MST on 2 December 1970, and reached a peak altitude of 190 km at +225 sec. A roll stabilized Attitude Control System (ACS) was used to point the telescope, and the position was monitored by an aspect camera. The path scanned in the sky from nose cone eject at 110 km (+110 sec) to +250 sec is shown in Figure 1. At +227 seconds a failure in the ACS system caused the payload to tumble for the remainder of the flight. The pointing direction of the telescope was determined from the aspect pictures until +250 seconds; only data obtained before this time is used in the analysis.

Results

(a) Backgrounds

Table I lists minimum fluxes observed during the flight. Also listed are the minimum signals with the contribution from scattered earthshine subtracted as described below. These are thus the minimum signals detected in the flight and as such are upper limits to the celestial background.

The earth, if viewed directly by the telescope, is approximately 10^8 times brighter in the $5\mu \leq \lambda \leq 23\mu$ range than the upper limits in Table I, so the contribution of scattered terrestrial emission to the signals may be sizable even for a well baffled system. Therefore knowledge of the baffling function (i.e. beam pattern) of the optical system is required. Because the telescope is helium cooled and cannot be opened in the atmosphere, the baffling functions for the detectors could not be measured under flight conditions. Instead, the baffling was calibrated in the laboratory, with the instrument at room temperature, and using visible light. At large zenith angles the observed flux vs. zenith angle curve agrees well with that obtained by convolving the calibrated baffling function with the geometry of the earth for the Ge:Ga detector. For the three Ge:Cu detectors the slopes agree well, however the measured radiation is about a factor of 10 lower than that predicted. Figure 2 shows the observed flux as a function of zenith angle for the 16-23 micron detector. BB' is the computed baffling function fitted to the data at very large zenith angles. This plot is typical of all the detectors.

(b) Zodiacal Emission

During the period from +200 sec to +250 sec, there is more diffuse radiation at small zenith angles and all wavelengths than that predicted from scattered earth light. A number of individual sources were also observed and the reduction of these data is in progress. In Figure 2 this excess diffuse radiation is plotted versus zenith angle for the 16-23 micron detector. Because the field of view of each detector is $1\frac{1}{2}^{o}$ x $1\frac{1}{2}^{o}$ square and the uncertainty pointing direction is $\sim 1/2^{o}$, we consider it significant that all the excess fluxes in pass 2 peak within 2^{o} of the ecliptic plane. Figure 3 shows plots of excess flux vs. ecliptic elevation angle for the 12-14 micron and 16-23 micron detectors.

The scanning pattern of the flight took the telescope across the ecliptic plane twice during the flight. During the first pass, dust particles carried up with the vehicles appear to have been drifting across the field of view of the detector. (Local dust grains are recognized by their large signal size, apparent spinning motion, velocity and spin rate consistency and simultaneous appearance on all channels.) The smallest signals observed within 5^{o} of the ecliptic plane on pass 1 (Table I) are presented as upper limits.

There does not appear to be a correlation between the excess flux observed in the second scan and the rocket altitude for any detector. The slow variation of signal with time seems to rule out dust grains, carried up with the vehicle, as the source. We cannot positively rule out upper atmospheric emission as a source of some of the flux observed. The fact that the excess flux reached a maximum within 1/2 km of the maximum altitude of the rocket, for all the detectors, is a strong argument against its origin being in the upper atmosphere.

Discussion

The estimates of emission from the ecliptic plane are listed in Table I and plotted in Figure 4. Our upper limits from scan 1 are consistent with the data from scan 2. In what follows, only the data from scan 2 will be used. For the $70\mu \leq \lambda \leq 130\mu$ band no attempt has been made to correct for contribution from a galactic background. This could lower the quoted value by a significant fraction (Pipher, 1971). The Ge:Ga detector is sensitive to emission from zodiacal particles at larger distances from the sun (cooler particles) than are the Ge:Cu detectors. These two effects would tend to raise this point above a blackbody curve drawn for the 3 Ge:Cu detectors.

Taking the observed upper limits from the second pass, one can roughly calculate the total thermal emission of the zodiacal particles. For blackbody emitters at a temperature ranging from $230^{\circ}K$ to $350^{\circ}K$, the flux in the 12-14 micron band is $(11 \pm 1/2)\%$ of the total emitted energy, so our estimate of the total emitted flux of 1.2×10^{-9} watts/cm^2 str is quite insensitive to grain temperature. This flux can be compared with the scattered visible radiation at the same elongation angle, $\epsilon \sim 160^{\circ}$, of $\sim 2 \times 10^{-10}$ watts/cm^{2}str

(Allen, 1964). If one assumes that the grains scatter isotropically, with an added fraction α in the forward and backward directions

$$\alpha = \frac{\text{Flux scattered forward+backward}}{\text{Flux scattered isotropically}}$$

then the total flux scattered by the grains is $(1-\alpha)x2x10^{-10}$ watts/cm^2 str. Then the ratio of these two fluxes, i.e. $\frac{\text{Flux scattered}}{\text{Flux emitted}} = \frac{\text{Solar Flux scattered}}{\text{Solar Flux absorbed}}$ is $\sim 0.15(1+\alpha)$. With $\alpha \sim 1$ this ratio becomes $\sim .3$ which is not unreasonably large for typical particles. These results are derived assuming blackbody emission by the radiating particles. The total flux emitted should not be strongly affected by a nonconstant (in λ) emissivity, as long as particles have diameters of 2.5μ and larger.

As a comparison, recent infrared observations of comet 1969g and comet 1969i by Kleinmann, et al. (1971) yield a ratio of total scattered to total absorbed solar flux in cometary nuclei of 0.3 to $0.6(1+\alpha)$ where α is the same parameter defined above. This total scattered sunlight was determined by fitting a solar spectrum to the data of Kleinmann et al. (1971) in the 1.25-1.6μ region (we assumed that the observations were made at sufficiently large elongation angles that contributions to the scattered light from a forward scattering lobe would be negligible). The emitted radiation was determined by integrating their results for $5\mu \leq \lambda \leq 60\mu$. (Where no 1.25μ and 1.65μ data were presented, the ratio $\frac{I(1.65\mu)}{I(2.2\mu)}$ was assumed to be constant.)

Summary

Upper limits to the diffuse background radiation in the intermediate infrared ($5\mu \leq \lambda \leq 23\mu$), as measured from a sounding rocket, are presented. An excess signal was observed from the direction of the ecliptic plane, and is attributed to thermal emission from the interplanetary medium. It is possible that the minimum signals observed in the flight also can be accounted for by the same emission mechanism, since the minimum signal was observed near (i.e. within 20°) the ecliptic plane.

Acknowledgments

It is a pleasure to acknowledge Mrs. J. L. Pipher for assistance in the preparation of the payload and analysis of the data. Excellent technical assistance was provided by Mr. G. Stasavage. The efforts of our subcontractors, H. Kondracki of Pan Monitor, Inc., and W. Wernsing and R. Green of Williams Laboratories, Inc., are appreciated

The research reported on was sponsored by AFCRL contract F19628-70-C-0128.

References

Allen, C.W., Astrophysical Quantities, Second Edition, University of London, The Athlone Press (1964).

Harwit, M., Liege Symposium, 26, 506 (1964).

Harwit, M., Houck, J.R. and Fuhrmann, K., Appl. Opt. 8, 473 (1969).

Kleinmann, D.E., Lee, T., Low, F.J. and O'Dell, C.R., Astrophys. J., 165, 636 (1971).

Pipher, J.L., to be published (1971).

Pipher, J.L., and Houck, J.R., Appl. Opt. 10, 567 (1971).

Pipher, J.L., Houck, J.R., Jones, B.W. and Harwit, M.O., to be published, Nature (1971).

Quist, T.M., Proc. IEEE 56, 1212 (1968).

TABLE I

Detector	$\lambda(\mu)$	NEI(1),(2)	Min Detected Intensity(1)	Min Signal(1) -scattered earth light	Ecliptic Flux(1) Upper limit (pass 1)	(pass 2)
Ge:Cu	5-6	1.3×10^{-13}	3×10^{-11}	2×10^{-11}	$<6.5\times10^{-11}$	3×10^{-11}
Ge:Cu	12-14	8×10^{-14}	3×10^{-11}	2×10^{-11}	$<7.0\times10^{-11}$	6.0×10^{-11}
Ge:Cu	16-23	2.3×10^{-14}	1.8×10^{-11}	1.2×10^{-11}	$< 4\times10^{-11}$	2.5×10^{-11}
Ge:Ga	70-130	6×10^{-14}	1.4×10^{-12}	1.0×10^{-12}	$<1.4\times10^{-12}$	$< 9\times10^{-13}$

(1) Intensity watts/cm^2-str-μ

(2) Noise Equivalent Intensity

Figure Captions

Figure 1 Scan path of telescope (in ecliptic coordinates, ϵ is elongation angle, α is elevation angle) from nose cone and telescope cover eject until +250 seconds.

Figure 2 Intensity as a function of zenith angle for 16μ-23μ detector during the second crossing of the ecliptic plane. BB' is the contribution from scattered earthshine, to which the telescope responds in the following way. At small off-axis angles θ, there is a strong forward peak of half power width, $1\frac{1}{2}^{o}$ defined by the telescope's field stop. At larger angles, in the range shown, a function of the form $A \exp-(\theta/\theta_o)$, with $A \sim 10^{-3}$ and $\theta_o \sim 8^o$ represents the telescope response. The main contributions to this response come from radiation scattered by the telescope's black walls and subsequently scattered a second time by imperfections and dust on the primary mirror. We would expect the imperfections to scatter less at long wavelengths so that the near infrared off-axis response should be less than that measured for visible radiation in the laboratory. At longer wavelengths, around 100μ, our paint becomes less "black" (Pipher and Houck (1971)) and an increase in off-axis response is to be expected. These expectations are consistent with the inflight measurements.

Figure 3 Intensity as a function of ecliptic elevation angle for 12μ-14μ and 16μ-23μ detectors (with scattered earthshine subtracted, as explained in the caption for Fig. 2).

Figure 4 Peak intensity during second pass across ecliptic plane, as a function of wavelength (scattered earthshine subtracted).

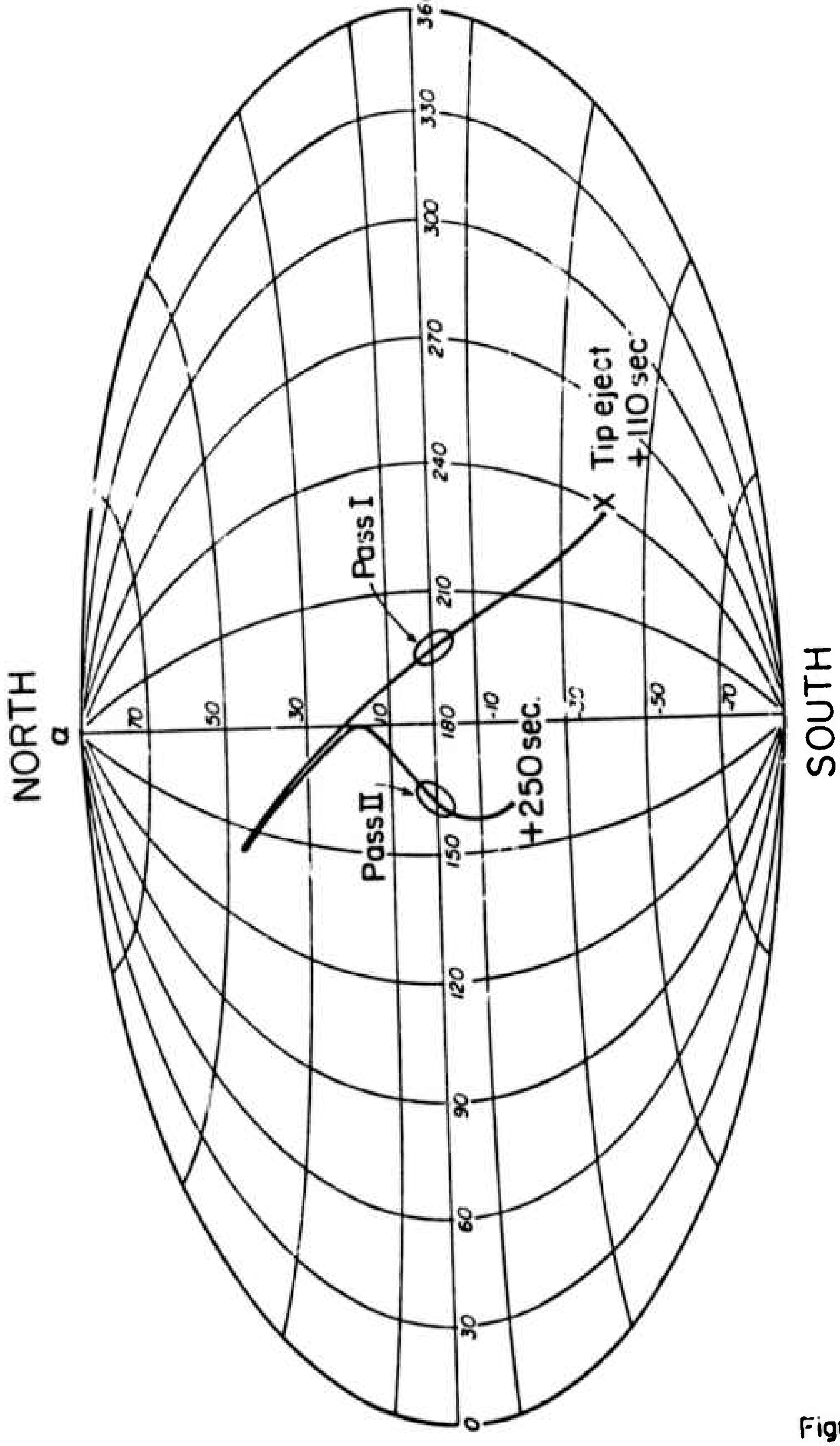
NORTH
α
SOUTH
Pass I
Pass II
Tip eject
+110 sec
+250 sec.
360
330
300
270
240
210
180
150
120
90
60
30
0
70
50
30
10
-10
-30
-50
-70

Figure 1.

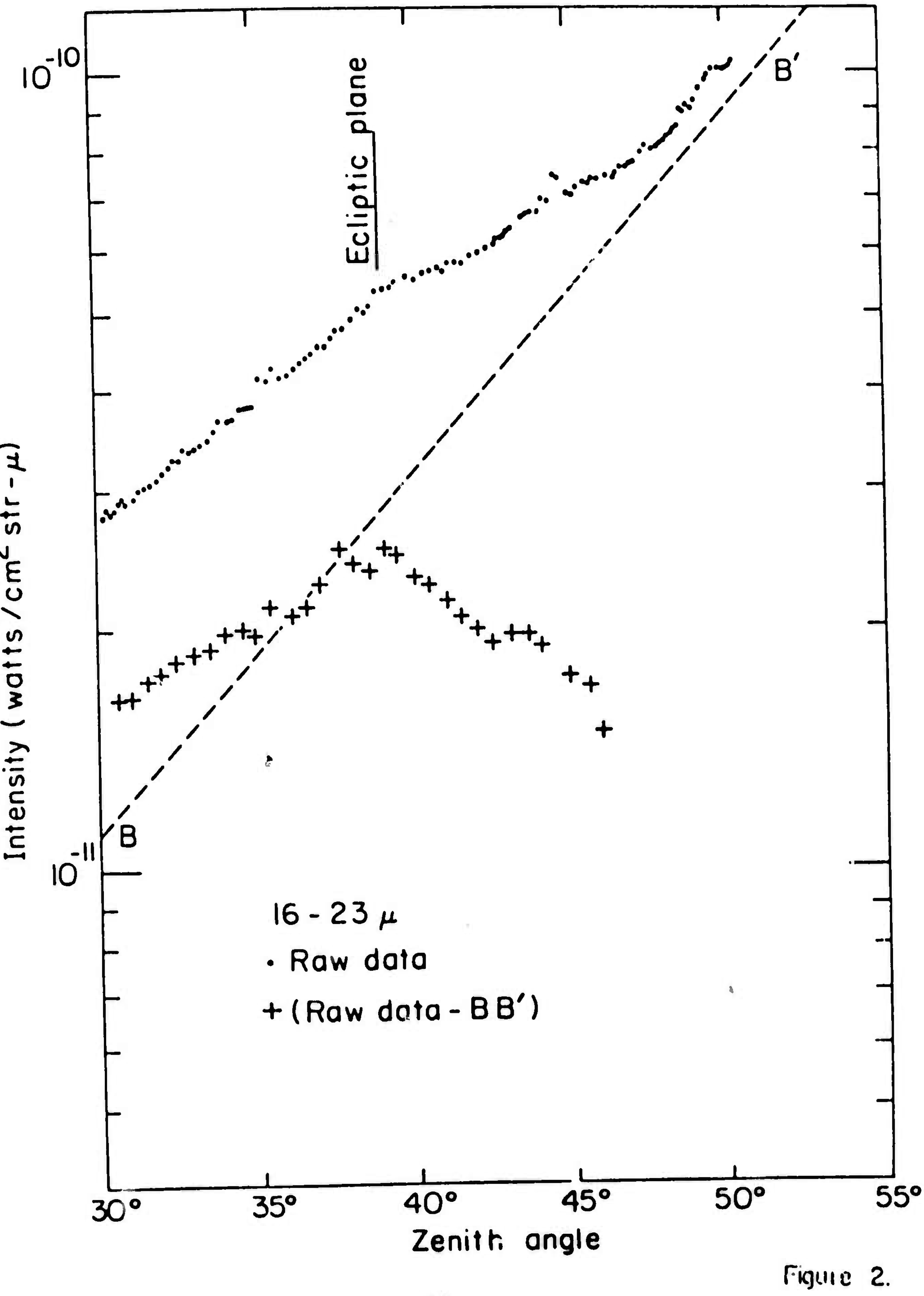

Ecliptic plane
B'
B
10^{-10}
10^{-11}
Intensity (watts /cm^2 str - μ)
16 - 23 μ
• Raw data
+ (Raw data - B B')
30°
35°
40°
45°
50°
55°
Zenith angle

Figure 2.

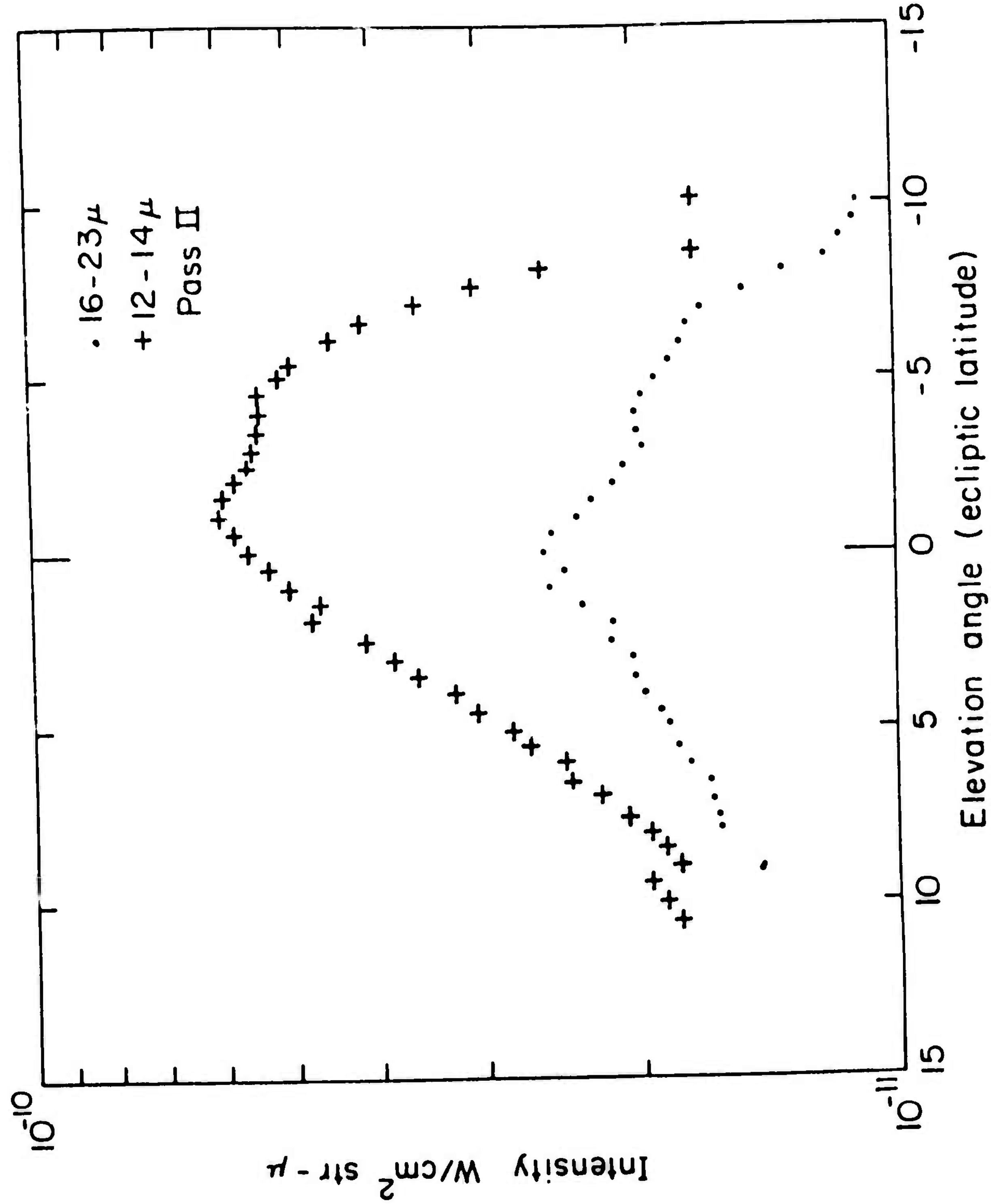

· 16-23μ
+ 12-14μ
Pass II
Elevation angle (ecliptic latitude)
Intensity W/cm^2 str - μ
10^{-10}
10^{-11}
15
10
5
0
-5
-10
-15

Figure 3.

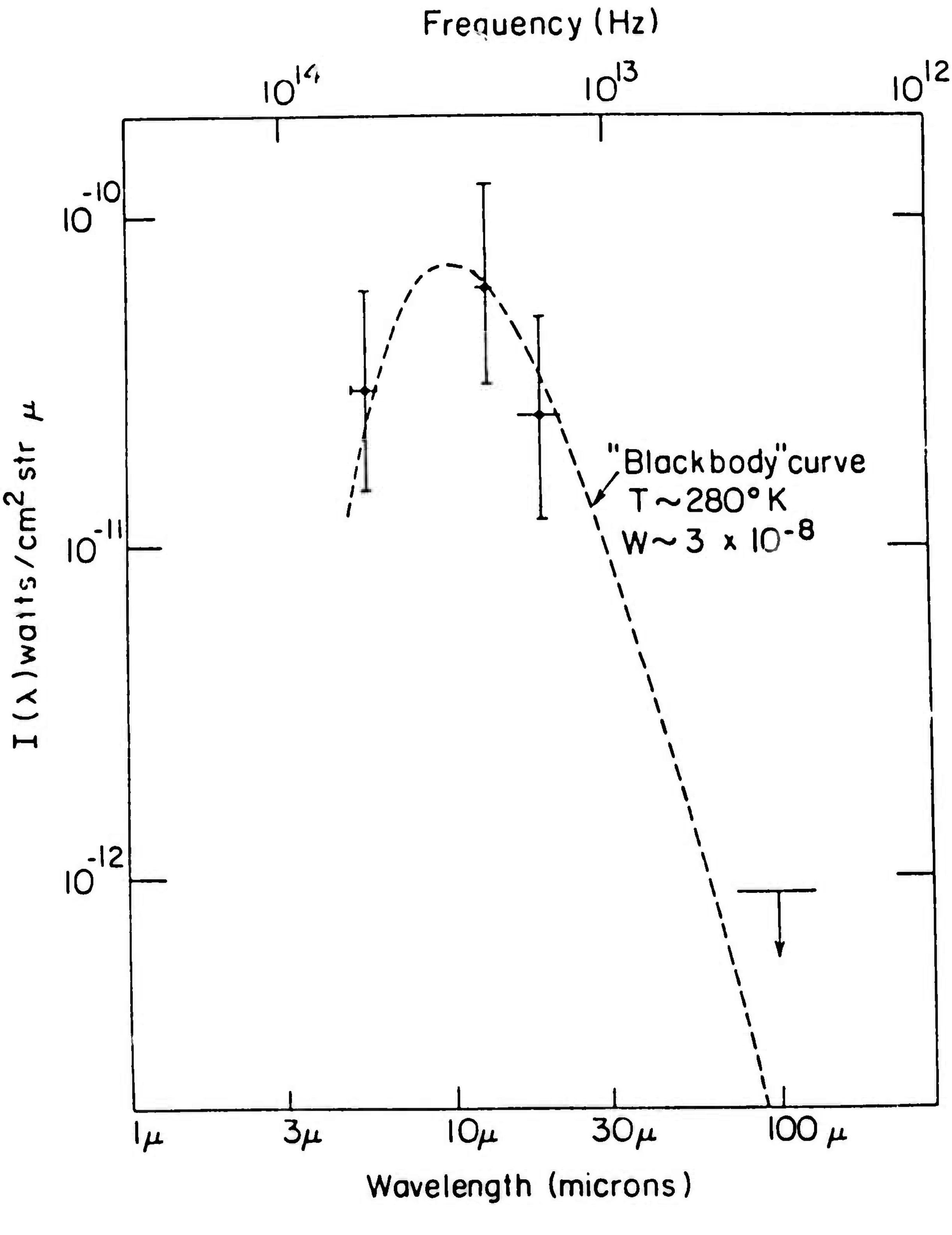

Frequency (Hz)
10^14
10^13
10^12
10^-10
10^-11
10^-12
I (λ) watts/cm^2 str μ
"Blackbody" curve
T ~ 280° K
W ~ 3 x 10^-8
1μ
3μ
10μ
30μ
100 μ
Wavelength (microns)

Figure 4.

Section II. ROCKET MEASUREMENTS OF THE GALACTIC BACKGROUND AT 100μ

Judith L. Pipher+

ABSTRACT

Measurements of the diffuse background radiation in the 85-115μ band are presented, as observed from altitudes close to 190 km with a rocket-borne, liquid helium cooled telescope. Evidence is given for detection of the galactic background due to thermal grain emission at galactic latitudes of 5-35°, and at a galactic longitude of ~ 163°. At small latitudes, the background intensity is measured to be ~ 9 x 10^{-11} watts/cm^2-sr; the average number density of grains derived is consistent with the optically determined measure. The 100μ data is compared with 20μ data taken on the same flight, in order to draw some conclusions about the grain emissivity and temperature.

+Now at University of Rochester, Rochester, New York

INTRODUCTION

Recent observations[1-6] indicate that the galactic center, HII regions and dust clouds are strong infrared sources with peak intensity at 100μ. Although the mechanism for such emission is not perfectly understood (partially because there is a lack of far infrared data with good spectral resolution), absorption of ultraviolet and optical radiation by dust grains and subsequent re-emission in the infrared has been suggested as a possible source for all of the above objects. It has been recognized for some time that a diffuse galactic background should be observable in the far infrared due to the re-emission of galactic interstellar grains. Stein[7] first made rough predictions of the expected intensity. The temperature that the grains assume and the wavelength of peak emission depend on the heating machanism and the grain characteristics. Most models, however, predict that the galactic grain emission should peak in the 70-300μ range. The observed intensity will depend on the column density of grains along the line of sight, and will vary relatively slowly in brightness gradient. Since atmospheric constraints at wavelengths proximate to 100μ make differential chopping necessary even at balloon altitudes, it is possible only at rocket altitudes and higher to make wide field observations of diffuse galactic grain emission.

We report here observations of a diffuse galactic background, in the 85-115μ band, and give evidence that thermal grain emission is the most likely source of the radiation. The observations were made with a liquid helium cooled telescope carried above the atmosphere on Aerobee 170 rockets launched from White Sands. The observations reported here took place at about 01:32 MST on 1970 December 2, and some substantiation of these results were obtained from a flight at 21:35 MST on July 16, 1971. Preliminary results of the July flight were previously[1,2] reported as were more detailed accounts of the December flight.[8,9,10]

OBSERVATIONS

The cryogenic telescope used for the observations is described in reference 8 cited above. Although the main emphasis here will be on the 100μ (85-115μ) observations, reference will be made to the results from some of the other detectors flown.

On this flight, the telescope first scanned along the galactic plane, and then scanned perpendicular to the plane at an approximate galactic longitude of 163°. Because there were technical difficulties on the scan along the galactic plane, only the scan perpendicular to the plane will be discussed here, for galactic latitudes ranging from 5° to 35°. Because of an attitude control system (ACS) failure 225 seconds into the flight, the path was passed over only once. The raw data for this scan are presented in Figure 1 as a function of zenith angle. At zenith angles greater than 42^{o}, the contribution from scattered earthshine predominates over celestial signals. In order to obtain the celestial flux, the scattered earthshine component is subtracted from the raw data by the method outlined in references 9 and 10. Because the signal to noise ratio is large for these measurements, the major source of error is the absolute detector calibration, which is described in detail in reference 8. On the 1971 flight[1], 100μ observations of the galactic center agreed well with previous studies from balloon altitudes[2], giving added confidence in the calibration techniques. Another source of error is the subtraction of the scattered earthshine. At galactic latitudes less than 30^{o} this error is thought to be minimal. We estimate our subtracted intensity levels to be accurate to ± 50% close to the galactic plane. Figure 2 contains a linear plot of the difference data as a function of both galactic and ecliptic latitude. As can be seen, the mean intensity decreases with increasing latitude, and peaks as the ecliptic plane is crossed. As well, discrete sources, which can be identified with dark clouds, reflection nebulae[8], and an HII region[3,8] are superimposed on the background signal; these will be discussed in a separate article.

Unfortunately, it is not an unambiguous exercise to separate the galactic and zodiacal dust emission in the 100μ data shown in Figure 2. Soifer *et al.*[9] have measured the thermal emission from zodiacal particles at 5-6μ, 12-14μ and 16-22μ on this rocket flight. They find the spectrum of measured radiation in these bandwidths appropriate to a dilute 280°K blackbody. At these shorter wavelengths, the zodiacal emission has fallen in intensity by a factor of two to three by the time an ecliptic latitude of 10° is reached. For want of a more plausible model for the 100μ zodiacal component, similar scaling laws with ecliptic latitude are assumed. As discussed in the next section, galactic grain emission seems to be the most plausible explanation for the radiation that decreases in intensity with increasing galactic latitude, at $\ell^{II} \sim 163^\circ$. If the distribution of grains is approximately uniform, the radiation at 100μ should be optically thin. The total optical depth along the line of sight can be written as

$$\tau_{100} = \int n \, d\ell \cdot \pi a^2 \cdot \epsilon_{100} \tag{1}$$

where n is the number density of grains, $d\ell$ is an increment of path length along the line of sight, a is the grain radius, and ϵ_{100} is the emissivity of the grain at 100μ. For reasonable assumptions about the grain size and column density at $\ell^{II} \sim 163^\circ$, the small value of the 100μ grain emissivity for any plausible grain type ensures that the radiation is optically thin, and that a csc (b^{II}) scaling law should hold for the galactic grain emission for $b^{II} \geq$

5^{o} if one assumes a disc model of the Galaxy. An attempt was made to fit the data with a csc (b^{II}) law and the two adopted models of zodiacal emission, and the best fit curves are shown in Figure 2. The fit is fairly good for latitudes larger than 10^{o}, but the intensity falls off more slowly than csc (b^{II}) at small latitudes. This discrepancy reflects the inadequancies of a uniform disc model of the Galaxy. At zenith angles greater than 42^{o} the greatest errors in subtracting the scattered earthshine occur, and a discrepancy with adopted models is expected.

The July 197 flight was not designed to make galactic background measurements. The telescope first scanned south along the plane to the galactic center region. During this portion of the flight, the galactic emission in confused with the increasing horizon shine as the telescope points at increasingly larger zenith angles. In the region of the galactic center, not only does the horizon shine confuse observations of the background, but also the strong and extended sources at 100μ make observations of the background difficult. However, on a scan perpendicular to the plane, an ACS pointing error resulted in a crossing of the plane some 2-3^{o} away from the galactic center, beyond the extended 100μ source(1). As a consequence, the increasing intensity depicted at that time in Figure 3 is identified with thermal emission from grains. The detector field of view was 1 $1/4^{o}$, so that the galactic disc at 20 kpc would be smaller than the beam size. If the grain density typical of the solar neghborhood persists throughout the Galaxy within an order of magnitude, the total optical depth over this path length would still be less than unity. The intensity as the plane was crossed is some 30 times the value observed at $\ell^{II} \sim 163^{o}$ and $b^{II} = 5^{o}$. This intensity, within reasonable error, corroborates the December 1970 observations reported here.

POSSIBLE MECHANISMS FOR THE 100μ GALACTIC EMISSION

There are several possible mechanisms for production of the 100μ galactic emission. Thermal radiation from dust grains appears to be the most likely source.

By extrapolation from the radio data, several authors(11,12) have shown that synchrotron radiation, Inverse Compton radiation and free-free emission are not expected to be strong sources of 100μ radiation, and in fact are all at least an order of magnitude down in strength from the observed signal in the galactic anticenter direction close to the plane. Synchrotron emission in the far infrared as the primary energy(13) requires moderately high magnetic fields; normal synchrotron emission not only would require high magnetic fields(14) but also a low frequency galactic absorption mechanism to reconcile the radio data with the 100μ data. The density of relativistic electrons required by an Inverse Compton mechanism is too high.

Fine structure line emission in the Galaxy is expected to be of limited concern in the 85-115μ band(15). The only possible candidate, the 88.16μ line of O III, is predicted to be strong only in HII regions. Hence, this mechanism is not considered likely.

Molecular line radiation in the 85-115μ band, or resonance radiation from oscillators trapped in grains are possible sources of the 100μ galactic background. The latter possibility is the more likely; however, without observations with increased spectral resolution, a specific model will not be examined in detail.

The mechanism of thermal emission from dust grains within the Galaxy seems to be the most attractive possibility. The observed energy density of the 100μ radiation ($4\pi I/c$ where I is intensity) close to the plane is $3 \pm 1.5 \times 10^{-13}$ ergs cm^{-3}. This number should be compared with the energy density in starlight, including the near IR sources, 8×10^{-13} ergs cm^{-3} (16). The similarity of these energy densities lends credence to the idea that efficient absoprtion of starlight by the grains and subsequent reemission at a wavelength dependent on the temperature the grains assume (which in turn depends on the size and type of grain) accounts for much of the radiation produced in the far infrared.

Because interstellar grains are thought to be small (0.05μ-0.2μ in radius) they cannot emit efficiently at $\lambda >> 2\pi a$ where a is the grain radius. The far infrared emissivity falls off approximately as $1/\lambda^{\beta}$ where β is thought to lie between 1 and 2. (See, e.g. reference 17.) The specific wavelength dependence is a function of the grain composition, and the interstellar medium may very well contain a range of grain sizes, shapes and compositions. The 'free space' temperatures that the grains can attain are given by the radiative equilibrium of the grains with their environment

$$\int_0^\infty R(\lambda)\epsilon(\lambda)\, d\lambda = \int_0^\infty \epsilon(\lambda)\, B(\lambda, T_g) d\lambda \qquad (2)$$

where T_g is the grain temperature, $\epsilon(\lambda)$ is the emissivity of the grain, radius a, at wavelength λ, $B(\lambda, T_g)$ is the Planck distribution of temperature of the grain, $R(\lambda)$ is the radiation field of the environment. The two integrals in equation (2) generally refer to different wavelength regions. For grains in free space, or in clouds of moderate opacity, the ultraviolet optical and near infrared wavelengths dominate the left hand side of the equation, while the low grain temperatures attained imply that the right hand integral covers far infrared wavelengths. If F is the flux of energy, in watts/cm^2, emitted from a grain surface in the 85-115μ bandwidth, then under the assumption of isotropic emission and a single grain size, the intensity observed at earth above the atmosphere along a line of sight is

$$I_{100} = F \cdot a^2 \cdot \int n \, d\ell \qquad (\text{watts/cm}^2\text{-sr}) \qquad (3)$$

Because the actual parameters describing galactic grains are quite uncertain, several extreme models of grains are considered here. F was calculated for these models, using free space grain temperatures and infrared emissivities appropriate to the grain, and assuming the stellar radiation field as the sole source of grain heating. A single representative grain size was adopted for each model. The important grain size ranges have been given by Greenberg[17] as

$$a_{ice} = 0.05\text{-}0.3\mu$$

$$a_{graphite} = 0.05\text{-}0.1\mu$$

$$a_{silicate} = 0.05\text{-}0.1\mu$$

$$a_{core} = 0.05\mu$$

$$a_{grain} = 0.1\text{-}2.0\mu \text{ for core-mantle grains .}$$

The value of I_{100} is 9×10^{-11} watts/cm^2-sr, and corresponds to a total path length along the line of sight of roughly 1 kpc. On the assumption of a uniform distribution of grains along this path, the average number density of grains was calculated. These values are tabulated along with the relevant grain parameters in Table I. Silicate grains are not included, because the far infrared emissivities for such grains are very uncertain[18]: it is expected that the column and number densities derived for the silicate grains would be larger than those for the ice grains, because the grain temperature expected ($\sim 9^{\circ}$K) shifts much of the radiation out of the detector bandwidth.

TABLE I

Grain Type	$T_g(^oK)$	a (μ)	$\int nd\ell$ (cm^{-2})	$\bar{n}(cm^{-3})$	Source of Grain Parameters
pure graphite	43	0.05	$4x10^{10}$	$1.3x10^{-11}$	ref. 19
dirty ice	15	0.2	$2x10^9$	$7x10^{-13}$	ref. 7
core-mantle	17	0.05, 0.15	$2x10^9$	$7x10^{-13}$	ref. 17, 19

Both the dirty ice and core-mantle grain models give reasonable agreement with the optically determined measure of the average number density of 2×10^{-13} cm^{-3} (16). Impure graphite grains, and graphite grains with moderate numbers of resonances near 100μ (see eg., reference 19) could reduce the column density of grains required to produce the observed 100μ intensity, both because the grain temperature would be reduced, shifting the peak wavelength of emission closer to the acceptance band of the detector system, and because the resonance might fall within the band. Although such possibilities are interesting, detailed calculations do not appear to be warranted until further spectral information on the radiation becomes available.

DISCUSSION

It appears that pure graphite grains are excluded on the grounds that too large a grain density is required to give the appropriate 100μ intensity. In fact, graphite grains sufficiently pure to achieve a free space temperature of 43°K are not expected to exist in space. These grains are excluded on another ground as well. On the same flight, a 16-23μ detector was also flown. Using the grain column density from 100μ data, an intensity of 2.4×10^{-11} watts/cm^2-sr is predicted in this band due to thermal emission from pure graphite grains. The observed intensity, with the horizon-shine subtracted out, was at this time in the flight, 1.3×10^{-11} watts/cm^2-sr. At first glance, these values seem fortuitously close; however, Soifer et al.[9] have presented very convincing evidence that most if not all of this signal is due to zodiacal emission. As a consequence, we can conclude that the 16-23μ observation supports the conclusion that pure graphite grains are ruled out. The 16-23μ observations, however, are compatible with less pure graphite grains of free space temperatures of 33°K[17]; however, the column density of grains required by the 100μ observations is still rather high (~ 1×10^{10} cm^{-2}), and it is concluded tentatively that such grains are only marginally allowed by the observations.

On the other hand, core-mantle grains and dirty ice grains, attaining lower free-space temperatures, are attractive not only because of the more reasonable column density required to explain the observation, but also because an upper limit of 1.4×10^{-10} watts/cm^2-sr to the galactic emission observed at this time by a detector sensitive at

230-330μ, does not conflict with this conclusion.

We conclude that grain temperatures of 15-≤33°K are allowed by the observations for the grain types and sizes indicated. It is not a particularly restrictive conclusion; graphite grains with impurities and resonances can achieve temperatures within this range[19], as well as dirty ice and core-mantle grains. Wideband observations at 200μ and 40μ would do much to restrict the allowable grain types and temperatures. Narrow band measurements are required to define the role that impurity resonances play in grains.

ACKNOWLEDGEMENTS

The author would like to thank B. T. Soifer, M. Harwit and J. R. Houck for helpful discussions. She held a National Research Council of Canada Graduate Fellowship during the time the experimental work was executed.

The research reported on was sponsored by AFCRL contract F 19628-70-C-0128, and KPNO rocket branch supplied excellent support.

REFERENCES

1. Houck, J. R., Soifer, B. T., Pipher, J. L. and Harwit M., Ap.J. 169, L31 (1971).

2. Hoffmann, W. F., Frederick, C. L. and Emery, R. J., Ap.J. 164, L23 (1971).

3. Soifer, B. T., Pipher, J. L. and Houck, J R., to be published in Ap.J.

4. Harper, D. A. and Low, F. J., Ap.J. 165, L9 (1971).

5. Low, F. J. and Aumann, H. H., Ap.J. 162, L79 (1970).

6. Soifer, B. T., Ph.D. Thesis, Cornell University (1972).

7. Stein, W., Ap.J. 144, 318 (1966).

8. Pipher, J. L., Houck, J. R., Harwit, M. and Jones, B. W., Nature 231, 375 (1971).

9. Soifer, B. T., Houck, J. R. and Harwit, M., Ap.J. 168, L73 (1971).

10. Pipher, J. L., Ph.D. Thesis, Cornell University (1971).

11. Lequeux, J., Ap.J. 159, 459 (1970).

12. Partiridge, R. B., and Peebles, I. J. E., Ap.J. 148, 377 (1967).

13. Cavaliere, A., Morrison, P., and Pacini, F., Ap.J. 162, L133 (1970).

14. Burbidge, G. R. and Stein, W., Ap.J. 160, 573 (1970).

15. Petrosian, V., Ap.J. 159, 883 (1970).

16. Allen, C. W. Astrophysical Quantities, University of London, The Athlone Press, Second Edition, 1964.

17. Greenberg, J. M., Astron. and Astrophys. 12, 240 (1971).

18. Krishna Swamy, K. A., Ap.J. 163, 63 (1971).

19. Werner, M. W. and Salpeter, E. E., M.N.R.A.S. 145, 249 (1969).

FIGURE CAPTIONS

Figure 1. Signal level observed by 85-115μ detector as a function of zenith angle for a scan at $\ell^{II} = 163^o$, and b^{II} ranging from 5^o-35^o. Predicted horizon shine (earth scattering function and function used in data reduction) are shown.

Figure 2. Difference signal between raw data of Figure 1 and assumed horizon shine, as a function of galactic latitude, ecliptic latitude and zenith angle. A $\csc(b^{II})$ galactic emission and two zodiacal emission models are scaled so that their sum best fits the 100μ average background data. Discrete sources (corresponding to dust clouds, an H II region and nebulosity) are also evident.

Figure 3. Signal level observed by 85-115μ as a function of galactic latitude for a scan at $\ell^{II} \sim 2\overset{o}{.}5$, and b^{II} ranging from -5^o - $+5^o$. The horizon shine predominates over celestial signals except close to $b^{II} = 0^o$.

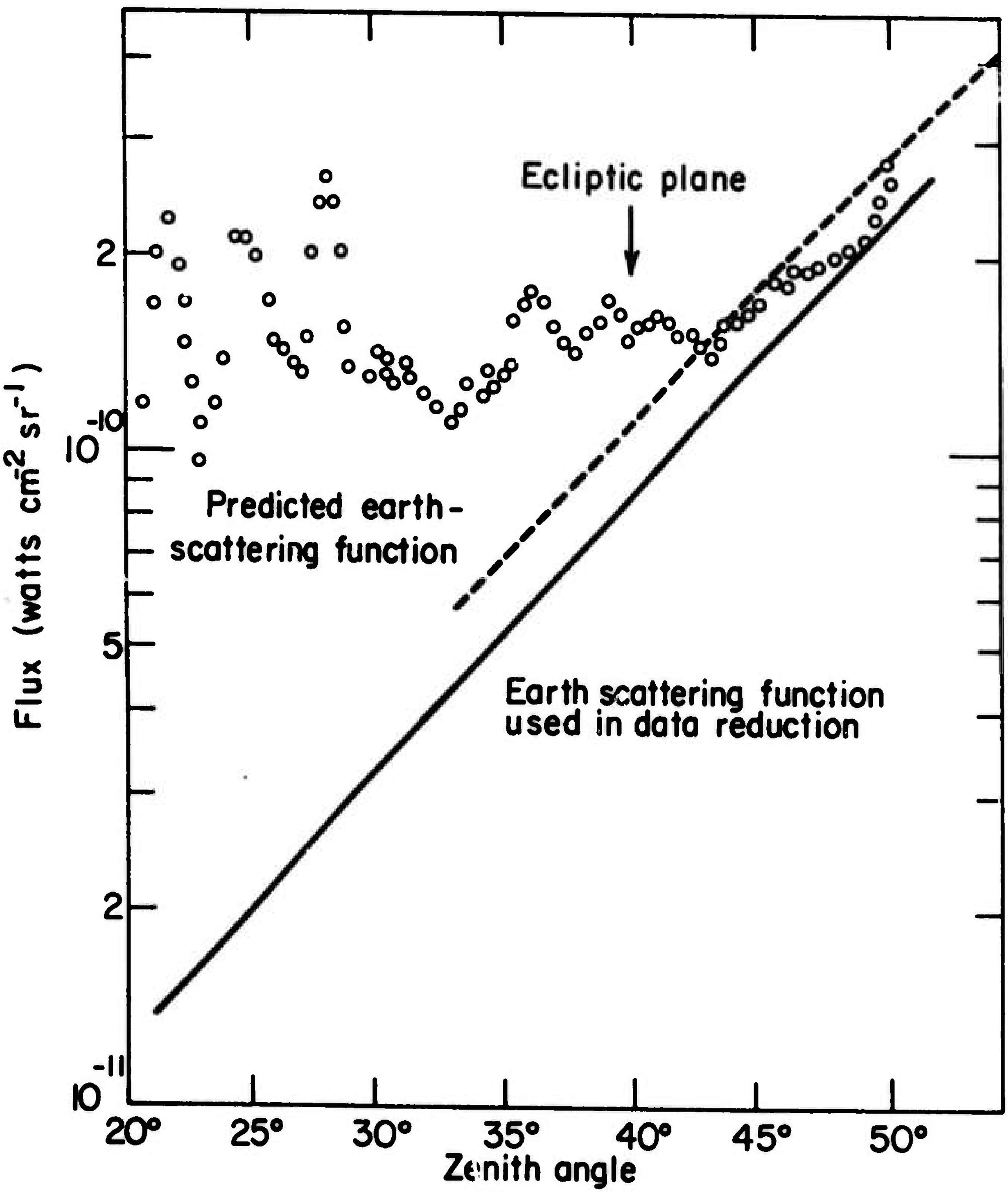
Ecliptic plane
Predicted earth-
scattering function
Earth scattering function
used in data reduction
Flux (watts cm^{-2} sr^{-1})
10^{-10}
10^{-11}
2
5
2
20°
25°
30°
35°
40°
45°
50°
Zenith angle

Figure 1

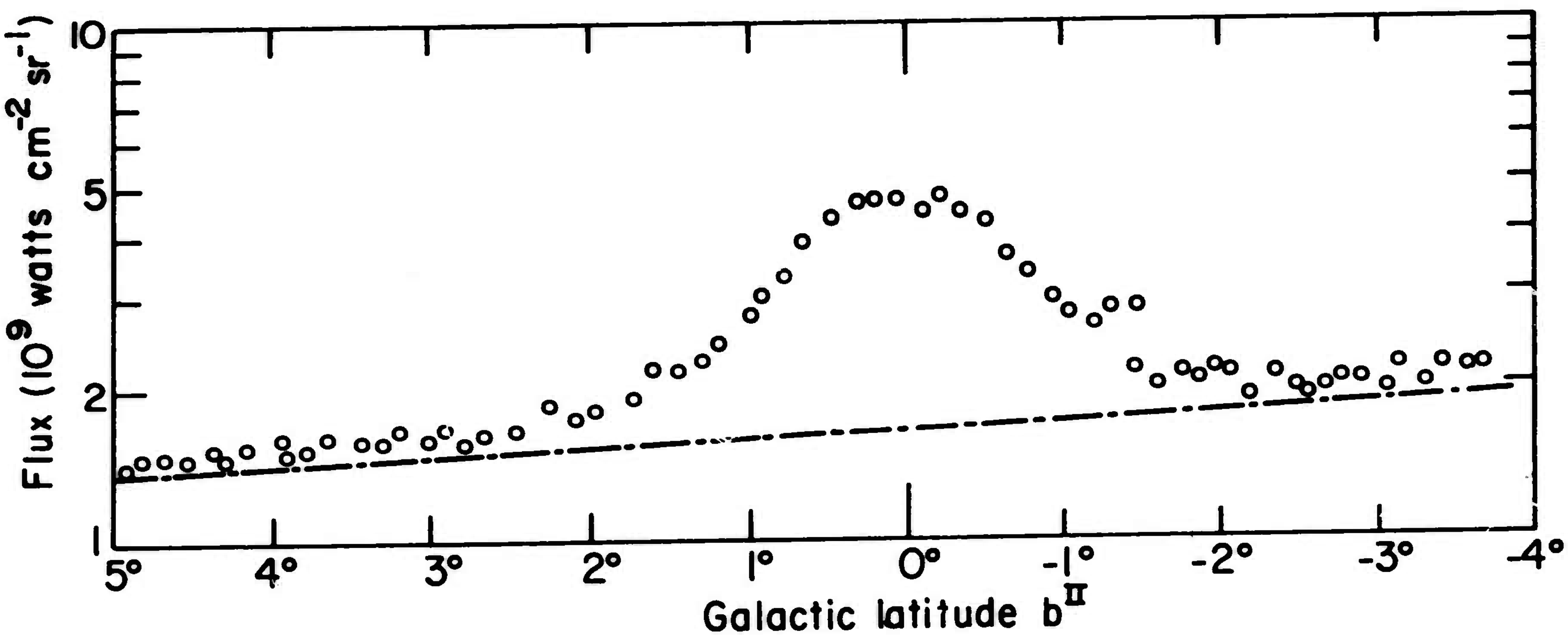
Flux (10^9 watts cm^{-2} sr^{-1})
10
5
2
1
5°
4°
3°
2°
1°
0°
-1°
-2°
-3°
-4°
Galactic latitude b^{II}

Figure 2

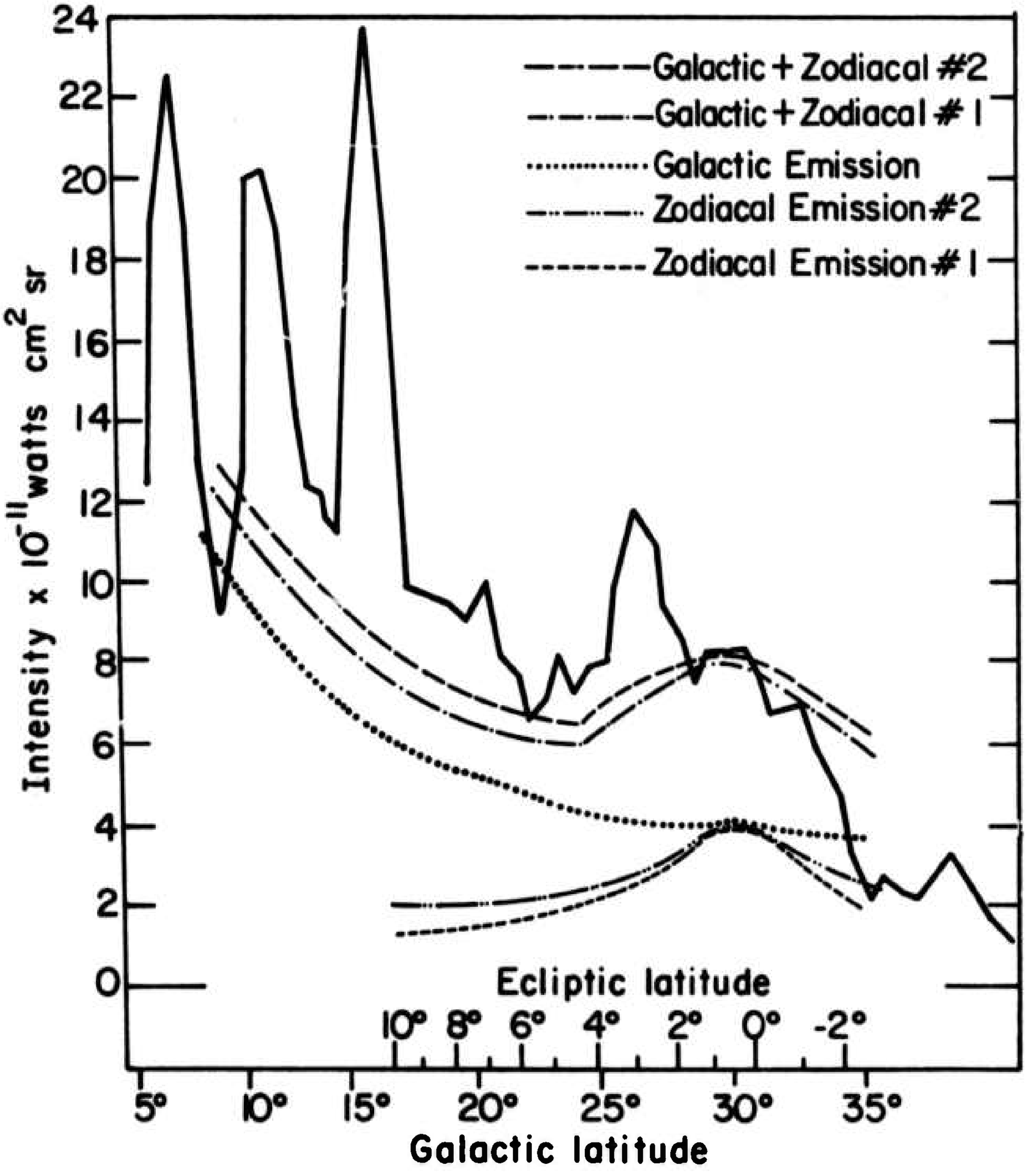

Galactic + Zodiacal #2
Galactic + Zodiacal # 1
Galactic Emission
Zodiacal Emission #2
Zodiacal Emission # 1
24
22
20
18
16
14
12
10
8
6
4
2
0
Intensity x 10^-11 watts cm^2 sr
Ecliptic latitude
10° 8° 6° 4° 2° 0° -2°
5° 10° 15° 20° 25° 30° 35°
Galactic latitude

Figure 3

Section III. ROCKET INFRARED 4-COLOR PHOTOMETRY

OF THE GALAXY"S CENTRAL REGIONS

J.R. Houck*, B.T. Soifer, Judith L. Pipher+

and Martin Harwit**

ABSTRACT

The central portion of the Galaxy was observed in the bandwidths 5-6, 12-14, 16-23 and 85-115μ during an Aerobee 170 rocket flight launched on July 16, 1971. We report on measurements made during a 100 sec time interval around 21:56 MST. In addition to the galactic center, we also observed four new sources.

+ Now at the Dept. of Physics and Astronomy, University of Rochester

* Alfred P. Sloan Foundation Fellow

** Visiting astronomer at Kitt Peak National Observatory, which is operated by the Association of Universities for Research in Astronomy Inc. under contract with the National Science Foundation.

On July 16, 1971, at 21:53 MST, an Aerobee 170 was launched from White Sands, N.M. The payload, consisting of a liquid helium cooled far infrared telescope, reached a maximum altitude of 190 km, and there were 280 seconds of useful observing time. We report here on 100 seconds of observations of the galactic center region, as measured by four infrared detectors with spectral bandwidths of 5-6, 12-14, 16-23, and 85-115μ. A more detailed report will be published later.

The telescope is similar to one flown previously (Harwit et al., 1969). It has an 18 cm diameter f/0.9 paraboloidal primary mirror. However, to avoid excess sensitivity to stray horizon radiation, secondary optics were added to improve the telescope beam pattern. These modifications will be reported elsewhere (Houck, 1971). They were considered necessary because the galactic center, as seen from a latitude 32°N, appears relatively low above the horizon. As in previous flights, the radiation was fully chopped by a tuning fork chopper, placed in the primary focal plane, and was then directed to the individual detectors through separate light pipes. This chopping procedure provided us with absolute flux levels for radiation coming from the individual 1/4° x 1° rectangular fields viewed by the different detectors (see Fig. 1). In order to see small changes in flux levels over and above the scattered earth shine background, the data was displayed both in terms of instantaneous flux changes as determined by means of a differentiating amplifier. The raw data from the differentiating amplifiers is displayed in Fig. 2.

Five sources were detected near the galactic center (cf. Table I). Only the strongest of these, the galactic nucleus, has been previously reported. Fig. 1 shows the scan pattern of our four detectors relative to the galactic center as mapped by Hoffmann _et al._ (1970) at 100μ. The instantaneous fields of view of our detectors, at different times in flight, are known relative to one another with an accuracy of the order of 0.1°. This data comes from photographs of the sky taken with an aspect camera. There is, however, some uncertainty in the absolute pointing direction relative to the direction viewed by Hoffmann _et al._ We have therefore obtained a best fit relative to their isophote map, by comparing our actual scan pattern to synthetic scans across the map (see Fig. 1). We obtain a unique fit which gives excellent agreement both of the absolute brightness detected at 100μ and of the scan pattern as we cross the galactic center. Fig. 1 shows this signal on our first pass through the center.

Table I lists the total flux measured in each bandwidth for each of the sources observed. The procedure used to obtain these fluxes, involves subtraction of the scattered earth shine component using the method of Soifer _et al._ (1971) and Pipher _et al._ (1971). Errors in absolute calibration are very hard to assess, in an experiment of this kind. We assign a somewhat arbitrary uncertainty to our values, amounting to $\pm$ 50%.

The flux attributed to source III, the galactic center, was computed in a way somewhat different from that used by Hoffmann et al. We only integrated the total flux detected by our detector. However, on the assumption that the map produced by Hoffmann et al. is correct -- and this appears to be true, at least for the portion through which we scanned -- we can extrapolate our data to obtain a flux value for the entire $3.6^{\circ} \times 2^{\circ}$ field covered by these authors. Our extrapolated value of 7×10^{-20} watt/m^2 Hz is in excellent agreement with their findings: a flux of 7.6×10^{-20} watt/m^2 Hz.

The agreement can be generally understood particularly because our galactic center measurements required very little background correction. In turn, this means that the differential chopping technique employed by Hoffmann et al. gives good flux levels, at least for this bright source. The general level of infrared emission from the galactic plane at 100μ does not appreciably contribute to the total flux reaching us from the central portions of the Galaxy.

Fig. 1 shows source II as a shoulder on source III -- the galactic center. This source was crossed by the 100μ detector on the scans made perpendicular to the galactic plane and actually appeared 20% brighter than seen in Fig.

2. It is this bigger flux which we list in the fifth column of Table I.

The fluxes measured for the galactic center by the short wavelength detectors are somewhat larger than those previously reported in the literature (Becklin et al., 1969 and Low et al., 1969). Because we are making absolute measurements, it is possible that a general background, not detected by the ground based observers added significantly to the measured flux.

We have no firm identifications for sources I and V, but a tentative assignment, respectively, to M8 and NGC 6357 seems reasonable on the basis of our aspect solution.

ACKNOWLEDGEMENTS

It is a pleasure to acknowledge the excellent support provided by Kitt Peak National Observatory's Rocket Branch Staff, directed by R. Nidey of KPNO. We also thank J. Labuda of Space General Corp., and R. Buck and staff of Oklahoma State University Research Foundation.

Outstanding technical assistance in the preparation of the payload at Cornell, and in the field, was provided by G. Stasavage of Cornell University, H. Kondracki of Pan Monitor, Inc. and R. Green.

The research reported on was sponsored by AFCRL contract F19628-70-C-0128.

References

Becklin, E.E., and Neugebauer, G., Ap.J. (Letters) 157, L31 (1969).

Hoffmann, W.F., Frederick, C.L., and Emery, R.J., Ap.J. (Letters) 164, L23 (1971).

Low, F.J., Kleinmann, D.E., Forbes, F.F. and Aumann, H.H. Ap.J. (Letters) 157, L97 (1969).

Pipher, J.L., Houck, J.R., Jones, B.W. and Harwit, M., Nature, 231, 375 (1971).

Soifer, B.T., Houck, J.R., and Harwit, M., Ap.J. (Letters) 168, L73 (1971).

Houck, J.R., To be published (1971).

TABLE I

Source	Total Flux (Watts/m^2-Hz)			
	5-6μ	12-14μ	16-23μ	85-115μ
I	$\leq 2.8 \times 10^{-24}$	1.8×10^{-23}	2.1×10^{-23}	6.2×10^{-21}
II	-	-	-	3.5×10^{-21}
III*	1.0×10^{-23}	5.1×10^{-23}	5.7×10^{-23}	5.7×10^{-20}
IV	$\leq 2.8 \times 10^{-24}$	1.6×10^{-23}	$\leq 1.5 \times 10^{-23}$	7.7×10^{-21}
V	4.4×10^{-24}	4.2×10^{-23}	6.5×10^{-23}	6.5×10^{-21}

*Galactic Center

Figure Captions

Fig. 1 Scan path of the detectors in Sagittarius region (cross hatched) superposed on Hoffmann's 100μ map of the Galactic center. The 100μ flux level as measured on the scan along the plane, in the direction of decreasing longitude is also shown. The fields of view of the four detectors, and their relation to the telescope optical axis are also indicated. The individual sources are labelled and referred to in the text. The galactic center is source III.

Fig. 2 The raw data for the four detectors. The data shown has been processed by a synchronous demodulator, a logarithmic amplifier, and a differentiating amplifier. This scheme enabled us to see point-like sources clearly, while rejecting slowly varying signals (such as the scattered earthshine). The sources are labelled as in Figure 1. Before 195 seconds, the detector passed over the sources in the sequence, 85-115μ, 5-6μ, 16-23μ and 12-14μ. After 195 seconds (reverse scan along the plane) this ordering is reversed. At 205 seconds, the scan perpendicular to the plane began, with no change in detector orientation.

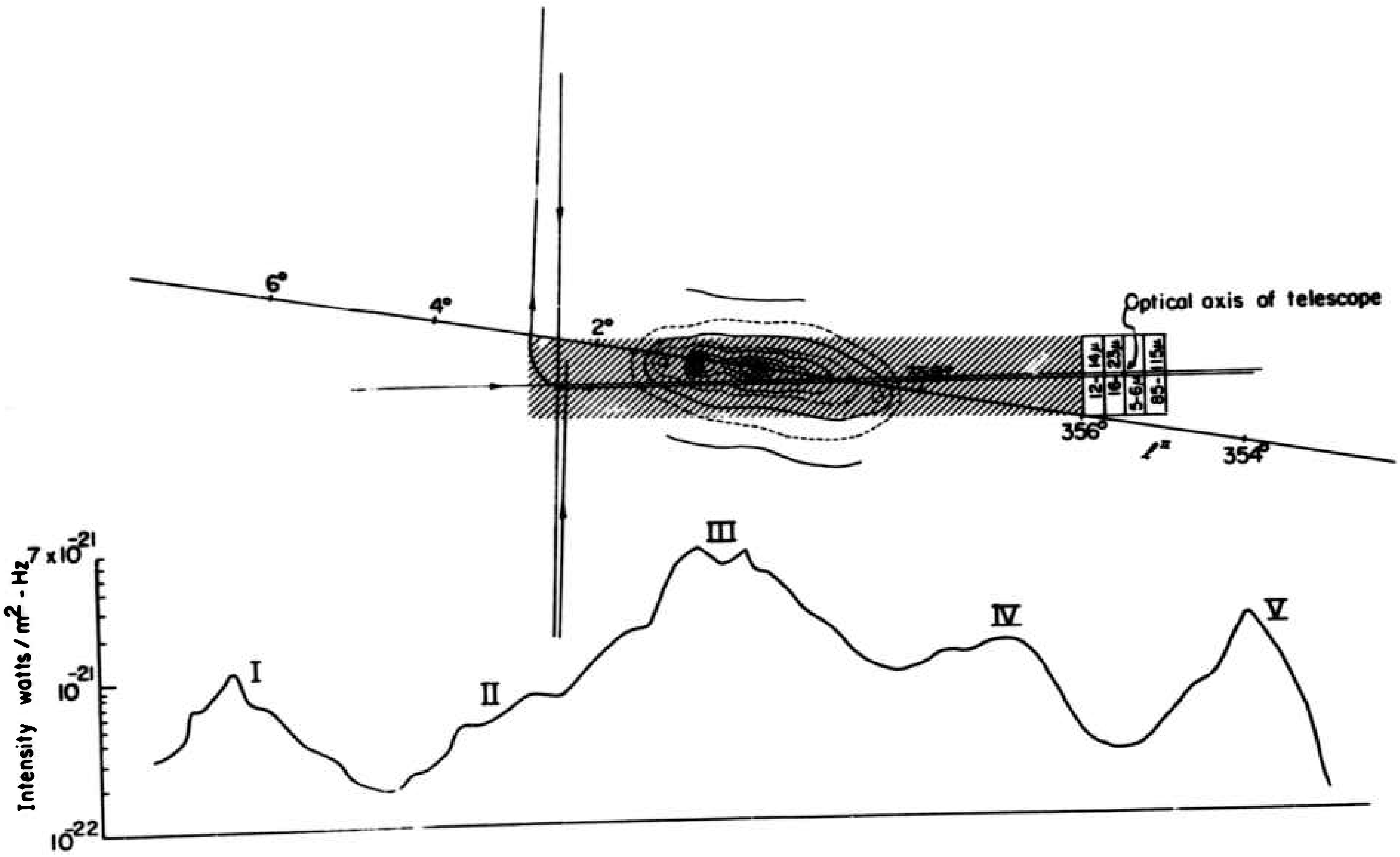

Optical axis of telescope
6°
4°
2°
356°
354°
12-14μ
16-23μ
5-6μ
85-115μ
I
II
III
IV
V
Intensity watts / m² - Hz
7 x 10⁻²¹
10⁻²¹
10⁻²²

Figure 1

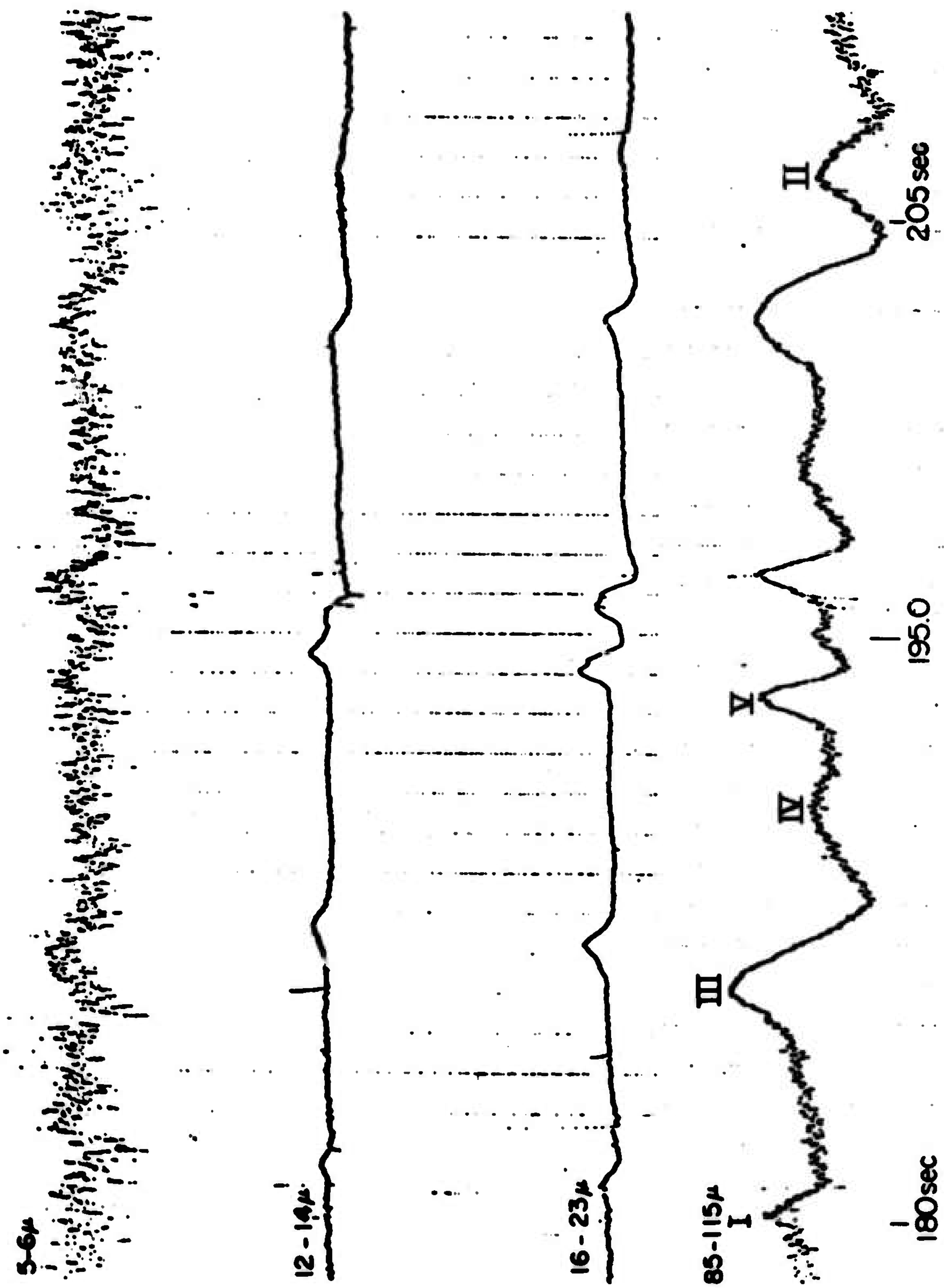

Figure 2

Section IV. THE FAR INFRARED AND SUBMILLIMETER BACKGROUND

J. R. Houck*, B. T. Soifer+ and Martin Harwit

and

Judith L. Pipher
Department of Physics and Astronomy
University of Rochester

ABSTRACT

We have repeated our earlier observations of the infrared and submillimeter background radiation. While the measured values of the infrared background radiation remain unchanged, we have failed to observe the high flux previously reported for the 0.4 to 1.3 mm range. This indicates that the flux cannot have been galactic or cosmic, but further observations are needed to rule out a solar cycle dependent geocoronal origin.

* A. P. Sloan Foundation fellow

+ Now at University of California, San Diego

An Aerobee 170 rocket was launched on flight KP 3.40 at 00:21 Mountain Standard time on July 18, 1972. At an altitude of 144 km above White Sands, New Mexico, the nose cone was ejected, and a liquid helium cooled telescope similar to one flown previously, started observing the sky in six wavelength bands 5-6, 12-14, 16-23, 85-115, 200-300, and 400-1300μ.

In this section we report the background radiation observed, and make a comparison with previous results. Earlier data reported by our group (Shivanandan et al., 1968, Houck and Harwit, 1969, Pipher et al. 1971) had set upper limits on a uniform background and had presented evidence for a relatively high background level at sub-millimeter wavelengths.

The submillimeter flux appeared isotropic and hence could not be attributed to simple atmospheric emission. If galactic or extragalactic in origin, the flux was barely consistent with X-ray background observations, (Hudson, et al., 1971) provided the X-radiation was produced by inverse Compton scattering of energetic electrons in the Galaxy. In addition restrictions on the spectral shape of an interstellar or extragalactic submillimeter flux were placed (Bortolet et al., 1969, Hegyi et al., 1972) by the low excitation states observed in interstellar atoms and by high spectral resolution mountain top (Mather et al., 1971, Nolt et al., 1972) and aircraft (Beckman et al., 1972) observations which detected only radiation that could be attributed to atmospheric emission. Other direct observations from rockets reported by the Los Alamos group indicated that the submillimeter flux would have to be at wavelengths less than 0.8 mm. Moreover, recent balloon observations by Muehlner and Weiss (1972) suggested that all their detected flux could be attributed to atmospheric emission.

In an attempt to settle such discrepancies, we have made a further measurement of the submillimeter background, but have failed to observe the earlier high signals.

In this flight instrumental changes were made to eliminate a number of possible sources of signal contamination have been discussed previously (Shivanandan et al., 1968, Houck and Harwit 1969b). Others were suggested to us by many colleagues.

1) Earth shine diffracted into the telescope at its open end;

2) Direct thermal radiation from the horizon which is multiply reflected inside the telescope;

3) The slow decay of oxygen atoms swept up as the rocket traverses the upper atmosphere. (These atoms can be trapped on cryogenically cooled surfaces, and atomic beam studies indicate that de-excitation of the electronic excited states occurs over times of the order of at least many minutes.) We are grateful to Dr. D. Offermann from

Bonn for bringing this effect to our attention;

4) Radiofrequency interference in the payload.

While calculations and experimental evidence argued against significant contributions by these effects, we nevertheless modified our liquid helium cooled telescope to be less sensitive to these types of interference. We did this by passing the observed radiation through additional field and aperture stops. A drawing of the optical system is shown in Figure 1.

We also minimized radio frequency interference by the use of additional shielding, changes in electronic circuitry, and elimination of both telemetry and radar tracking during a portion of the flight. During the entire flight including the 30 second period of interrupted telemetry and radar tracking all signals were recorded by an onboard tape recorder.

The tape record indicates that radio frequency and radar interference were not present on this flight. The data, however, also fail to reproduce the previously reported high submillimeter signals.

Our upper limit now is several times lower than the previously reported flux. The currently measured flux is slightly negative with respect to the $4.2^{o}K$ telescope temperature before the nose cone and telescope cover are ejected, at altitude. Its relative value is $-2 \times 10^{-10} \pm 2 \times 10^{-10}$ watt cm^{-2} sr^{-1}. The signal expected from a $4.2^{o}K$ telescope would be 3.6×10^{-10} watt cm^{-2} sr^{-1}. The actually observed signal coming from above the telescope therefore amounts to $1.6 \times 10^{-10} \pm 2 \times 10^{-10}$ watt cm^{-2} sr^{-1}. In the wavelength range between 0.4 and 1.3 mm, where our detector is sensitive, the expected flux from a $2.7^{o}K$ black background would be 0.4×10^{-10} watt cm^{-2} sr^{-1}. These levels are shown in Figure 2 and Table 1 which also give background radiation levels observed on this and previous Cornell University flights, and present the most recent data reported by other observers.

It is possible that improved stray radiation rejection could have eliminated the combined effects of the contamination sources 1, 2, and 3, listed above. In addition, effect 3 by itself should have been reduced by a factor of order three, since the telescope was opened at an altitude ranging from 25 to 36 km higher than on previous flights. A separate rocket flight would be required to isolate each of these sources of contamination.

While the many improvements in the apparatus would lead us to believe that the present observations, are, if anything, more reliable than those carried out in the past, it is worth noting that the detector field of view has substantially decreased with subsequent flights. At the present time, the focal plane aperture defining the field of view is only twice the diffraction limited size at the longest wavelengths in the acceptance band. Because our calibrations are most sensitive at the shortest wavelengths in the acceptance band, some small losses in efficiency in the actual background measurement are possible at the longest wavelengths. This effect is countered to some degree by an inverted cone feed to the detector, which acts as an efficient integrating cavity, particularly at the longest wavelengths. That our results are not substantially affected by diffraction losses is borne out by the following consideration: the field of view on the 1970 flight (Pipher et al., 1971) was only twice the present value, while on the earliest flights it was ~ 13 times larger. The 1970 result, while lower than the 1968-9 results by a factor of two, was certainly much larger than the present result although the aperture sizes are comparable.

It is also important to realize that a geocoronal effect cannot be ruled out by our current observations. The earliest measurements were taken at solar maximum, while all the more recent observations have been taken nearer minimum solar activity. We know of no specific mechanism which could be responsible for a geocoronal effect, but it is interesting that the Lyman-α geocorona has a flux of the order considered here, is only mildly anisotropic compared to limits that could be set with our instrumentation, and varies in brightness as a function of solar cycle.

While the present low submillimeter background observations are inconsistent with earlier flights, background measurements at other wavelengths are in good agreement with earlier data. The minimum signal observed at 100 microns is consistent with earlier values obtained by our group and by Los Alamos and NRL.

In earlier papers, (Harwit, Houck and Wagoner, 1970; Pipher, et al., 1971) we had pointed out that submillimeter background radiation flux levels give limitations on the amount of energy emitted by typical galaxies during past epochs.

The lower submillimeter signals now reported give even more stringent limitations, and indicate that the universe cannot have converted an appreciable fraction of mass into electromagnetic energy -- no more, at least, than fractions of the mass now visible in the form of galaxies. These results are shown in Table I.

On our present flight, Jupiter was detected twice in each of the four shortest wavelength bands. This had permitted us to recalibrate our flight instrument in terms of observations obtained by other observers, and gives us a calibration of background fluxes independent of our own laboratory blackbody calibrations. We find excellent agreement, using these two techniques. The principal uncertainties at 20μ and 100μ are in the quoted brightness of Jupiter in these wavelength bands. Since our earlier flights were carried out using the same blackbody technique, a satisfacotry cross-calibration relative to other infrared astronomical standards seems to have been established in this way (Aumann et al., 1969; Gillett *et al.*, 1969; and Low, 1966).

This work was supported by AFCRL contract F19628-70-C-0128.

We are grateful to R. Nidey and T. Avery of KPNO for their care and dedication to the project, and we thank G. Stasavage in our laboratory for excellent technical support.

References

Aumann, H.H., Gillespies, Jr., C.M., Low, F.J., 1969, Ap.J. 157, L69.

Beckman, J.E., Ade, P.A.R., Huizinga, J.S., Robson, E.I., Vickers, D.G., and Harries, J.E., 1972, Nature Physical Sciences 237, 154.

Blair, A.G., 1971, Nature Phys. Sci. 234, 26.

Blair, A.G., Beery, J.G., Edeskuty, F., Hiebert, R.D., Shipley, J.P., and Williamson Jr., K.D., 1971, Phys. Rev. Let. 27, 1154.

Bortolet, V.I., Thaddeus, P., and Clauser, J.F., 1969, Phys. Rev. Let., 22, 307.

Donahue, T.M., 1966, Ann. de Geophys. 22, 175.

Gillett, F.C., Low, F.J., and Stein, W.A., 1969, Ap.J. 157, 925.

Harwit, M., Houck, J.R., and Wagoner, R. V., 1970, Nature 228, 451.

Hegyi, D.J., Traub, W.A. and Carleton, M.T., 1972, Phys. Rev. Let. 28, 1541.

Houck, J.R. and Harwit, M., 1969a, Ap.J. Let. 157, L45.

Hudson, H.S., Peterson, L.E. and Schwartz, D.A., 1971, Nature 230, 177.

Low, F.J., 1966, A.J. 71, 391.

Mather, J.C., Werner, M.W., and Richards, P.L., 1971, Ap.J. 170, L59.

Muehlner, D. and Weiss, R., 1972, to be published.

Nolt, I.G., Radostitz, J.V., and Donnelly, R.J., 1972, Nature Physical Sciences 236, 444.

Pipher, J.L., Houck, J.R., Jones, B.W. and Harwit, M., 1971, Nature 231, 375.

Shivanandan, K., Houck, J.R., and Harwit, M., 1968, Phys. Rev. Let. 21, 1460.

Soifer, B.T., Houck, J.R., and Harwit, M., 1971, Ap.J. 168, L73.

TABLE 1

Wavelength	Flux (10^{-11} Watt $cm^{-2} sr^{-1}$)	Z	$\Delta\mathcal{E}/\rho_o c^2$	Source
5-6 μ	3	-----	[illegible]	Soifer et al., 1971
12-14	6	-----		Soifer et al., 1971
16-23	13	-----		Soifer et al., 1971
85-115	≤5	0.2-0.7	0.1	present data
130-200	<240	0.9- 2	9	Blair et al., 1971
200-450	8	2-5.5	0.6	Pipher et al., 1971
400-1300	<15*	5-17	3	Muehlner and Weiss, 1972
400-1300	12±20	5-17	2	present data
800-1200	<2*	10-16	0.4	Muehlner and Weiss, 1972
1200-1800	3			Muehlner and Weiss, 1972
800-6000	<15			Blair et al., 1971

*Corrected for atmospheric emission

Upper limits and measured values of infrared and submillimeter background radiation. At the three shortest wavelengths, the minimum observed flux may be due to zodiacal dust emission. The third column represents the wavelength shift required to bring a cosmic source emitting at 70μ, into the spectral range measured. The fourth column gives the maximum fractional mass that could have been converted into radiation at 70μ, by galaxies, during past epochs, without exceeding the observed flux. (cf. Harwit, Houck and Wagoner, 1970). The wavelength at which the emission of many infrared objects appears to peak is ~ 70μ.

Figure Captions

Figure 1 Optical system used on present flight.

Figure 2. Comparison of the Flux from a 2.7°K Blackbody with the Results of Various Experiments. Sources of the direct measurements are identified in Table 1. Interstellar molecular data are due to the NASA group (cf. Bortolet *et al.*, 1969), and Hegyi *et al.*

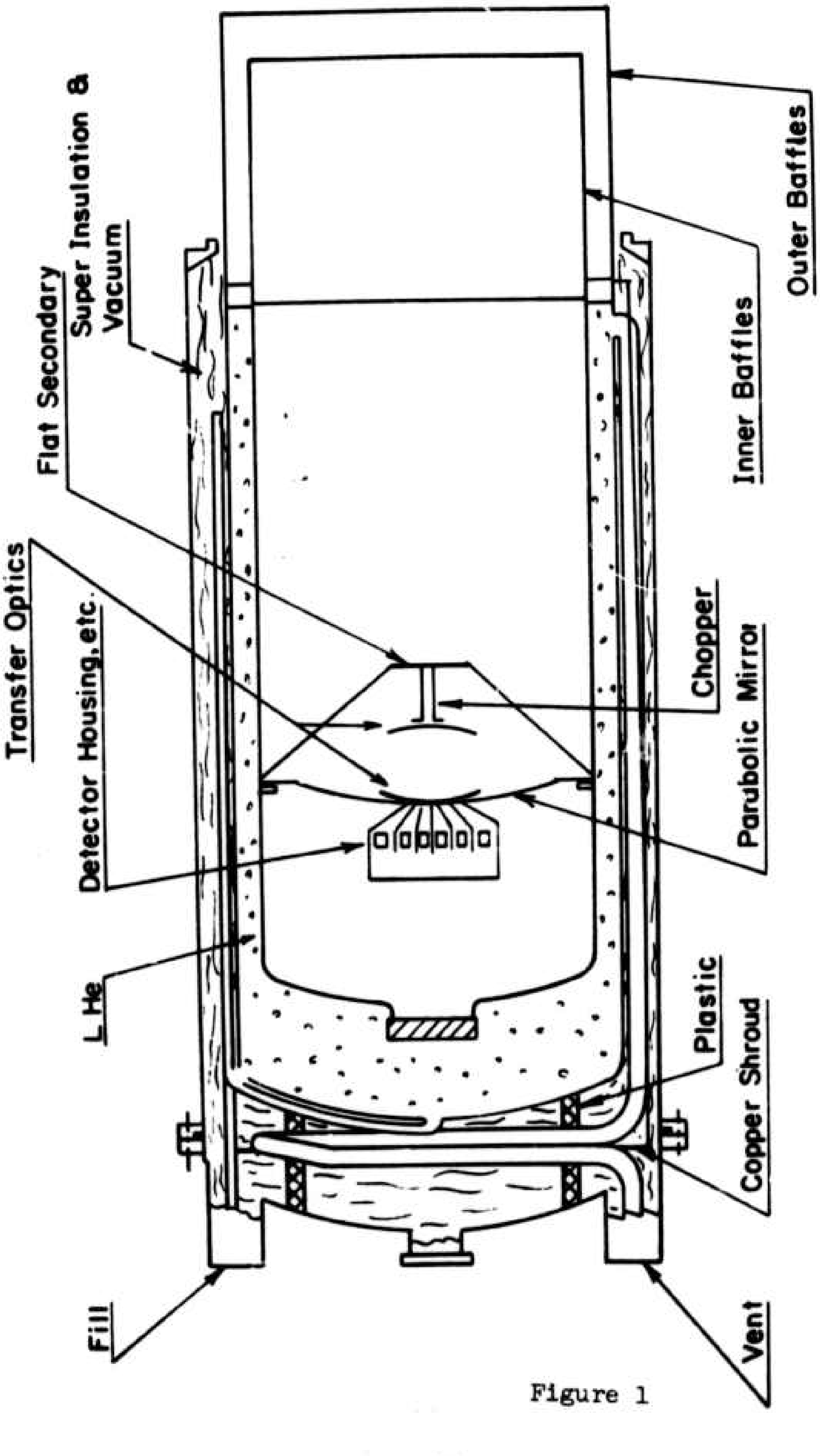

Super Insulation & Vacuum
Flat Secondary
Transfer Optics
Detector Housing, etc.
L He
Fill
Outer Baffles
Inner Baffles
Chopper
Parabolic Mirror
Plastic
Copper Shroud
Vent

Figure 1

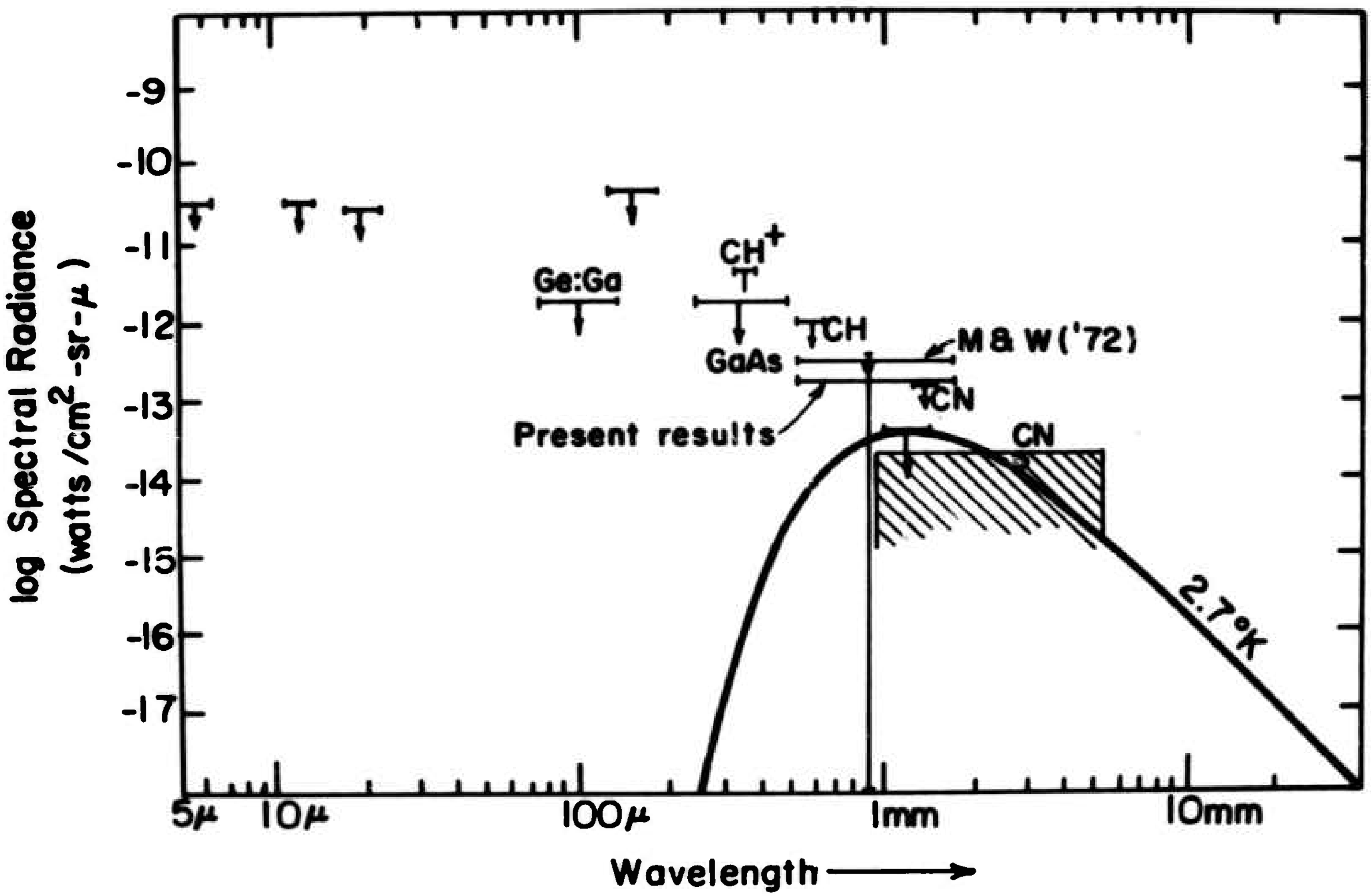
log Spectral Radiance
(watts /cm^2-sr-μ)
-9
-10
-11
-12
-13
-14
-15
-16
-17
Ge:Ga
CH$^+$
GaAs
CH
M & W('72)
CN
CN
Present results
2.7°K
5μ
10μ
100μ
1mm
10mm
Wavelength

Figure 2

Section V. GROUNDBASED INFRARED PHOTOMETRY

J. R. Houck and J. L. Pipher

During the contract period very high sensitivity copper coped germanium detectors were developed for the rocket telescope. We have used several of these detectors in a groundbased photometer for observations at 10 and 20μ. A photometer was built for use on the University of Rochester's 24" telescope at the Mees Observatory. The photometer employs an oscillating minor focal plane chopper. Provision is made for guiding continuously during the observations. An off set guider is also used to enable one to search blank fields searching for AFCRL Hi Star sources. Standard lockin and data recording procedures are used. The University of Rochester hopes to equip the telescope with a chopping secondary within the next year.

This is an ongoing program which is now being supported by the University of Rochester and the Sloan Foundation.